

Self-supervised Learning of Occlusion Aware Flow Guided 3D Geometry Perception with Adaptive Cross Weighted Loss from Monocular Videos

Fang Jiaojiao
995541569@qq.com

Liu Guizhong
liugz@xjtu.edu.cn

Abstract—Self-supervised deep learning-based 3D scene understanding methods can overcome the difficulty of acquiring the densely labeled ground-truth and have made a lot of advances. However, occlusions and moving objects are still some of the major limitations. In this paper, we explore the learnable occlusion aware optical flow guided self-supervised depth and camera pose estimation by an adaptive cross weighted loss to address the above limitations. Firstly, we explore to train the learnable occlusion mask fused optical flow network by an occlusion-aware photometric loss with the temporally supplemental information and backward-forward consistency of adjacent views. And then, we design an adaptive cross-weighted loss between the depth-pose and optical flow loss of the geometric and photometric error to distinguish the moving objects which violate the static scene assumption. Our method shows promising results on KITTI, Make3D, and Cityscapes datasets under multiple tasks. We also show good generalization ability under a variety of challenging scenarios.

Keywords—Self-supervised Learning, Depth estimation, Pose Estimation, Learnable Occlusion Mask

I. INTRODUCTION

Understanding the 3D scene structure from video sequences is a fundamental yet challenging computer vision task. With the development of artificial intelligence, there is a wide range of applications in autonomous driving, robotics, scene interaction, and augmented reality. The vision-based 3D scene geometry understanding has been studied extensively. The traditional methods mainly rely on the structure-from-motion (SfM) frameworks that leverage sparse hand-crafted features, and the multiple view geometry under the re-projection error [5]. However, these methods could only offer sparse results, and face difficulties in cases when the camera motion is degenerated. With the advent of deep learning, recently academics have tried to formulate a supervised deep convolutional neural network (CNN) based depth and pose learning framework. This produces satisfying results but suffers the inherent limitation of depending on large densely labeled training sets, which are difficult and laborious to obtain.

More recently, several authors [6] [7] focused on designing self-supervised systems and explored to learn the depth and pose networks without ground-truth by minimizing photometric loss among adjacent views. These systems implicitly embed basic 3D geometry and achieved competitive performance, but are still affected by occlusions, moving objects, and face difficulties in challenging scenarios. Due to the lack of accurate pixel correspondence between adjacent views in the occlusion areas, incorrect photometric loss would mislead the training process of all tasks in the self-supervised framework. The MaskFlowNet [8] learns to distinguish the occlusions by a learnable mask without any explicit occlusion signal supervision in the supervised optical flow learning and achieves better performance. Chen *et al.* proposed [9] a wonderful idea to deal with the dynamic nature

of the real-world scenarios in the self-supervised depth-pose learning framework by an adaptive photometric loss. Based on this brilliant thinking, we further consider the followings: 1) the reduced training data for both depth-pose and optical flow by the minimum error between them; 2) the occlusions, 3) the optical flow correspondences and camera pose-based epipolar geometric loss is sensitive to the moving objects.

In this work, we introduce an occlusion-aware optical flow-guided self-supervised depth-pose learning framework. We first explore to train the learnable occlusion mask combined optical flow network by the self-supervised manner with an occlusion-aware photometric loss. Then an adaptive cross-weighted loss of photometric and geometric error between the optical flow and the depth-pose is used to exclude the dynamic objects in calculating the training loss. Specifically, our main contributions are as follows:

i) To facilitate the self-supervised depth-pose learning, we import the mask flow network and explore to learn it in a self-supervised manner with an occlusion-aware photometric loss. Thus we can jointly learn the occlusion aware optical flow network and depth-pose networks in an end-to-end self-supervised manner and gain significant improvements on multiple tasks. Furthermore, we can obey the self-supervised nature of the existing depth, pose and optical flow learning framework, and automatically distinguish the occlusions for all tasks.

ii) The depth-pose estimation-based photometric loss will be invalid in the motion object region, while the optical flow based photometric loss is more robust in these situations. While the epipolar geometric constraints are just the opposite for depth-pose and optical flow in the area of motions. Thus in this paper, to improve the robustness of the model against moving objects, we consider the of photometric and geometric error simultaneously to construct an adaptive cross weighted loss between the depth-pose and optical flow.

The proposed framework is extensively evaluated on the KITTI dataset, and gains over the state-of-the-art methods without on-line refinement. Fig. 1 shows the overview of our proposed method.

II. RELATED WORKS

The vision-based 3D scene understanding encompasses many basic tasks such as depth estimation, optical flow, visual odometry, etc [9]. Traditional feature matching and structure-from-motion (SfM) based methods [4],[5] had a mature mathematical theory system and achieved remarkable results. But the reconstruction results were often sparse and prone to error in low-texture or occluded areas.

To address the bottleneck of sparse hand-crafted feature matching, recent methods focused on deep-learning based scene geometry understanding via a lot of dense labeled ground-truth data and had been successfully applied to many tasks, such as monocular depth estimation [13],[14], optical

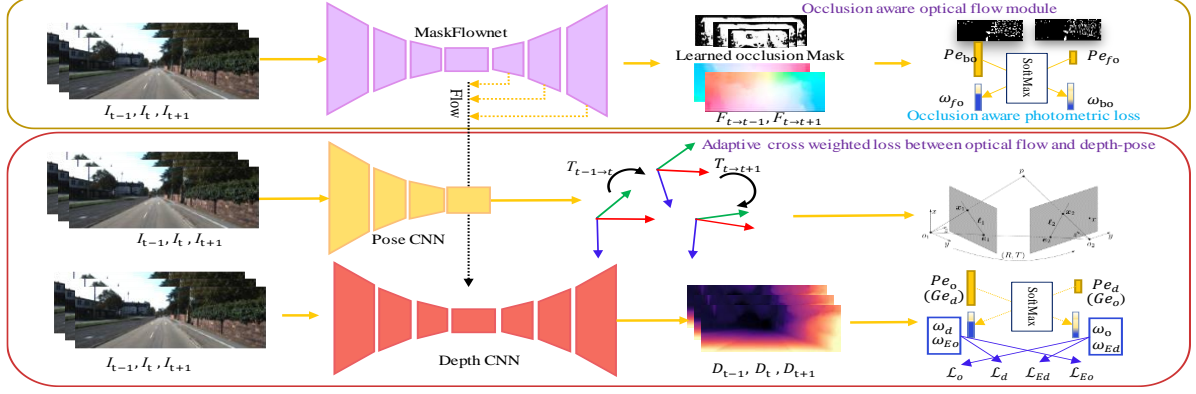


Fig. 1. Overview of the proposed framework. Our model imports the learnable occlusion mask optical flow into the self-supervised depth-pose learning framework. Then an adaptive cross weighted loss is used for the end-to-end self-supervised depth-pose and optical flow learning.

flow [16],[17],[18] and camera pose estimation [20],[21]. These methods relied on expensive specialized equipment (e.g. LIDAR) for data collection [1], [2] and formulated as a pure regression problem that cares little about geometric relations. To make use of the multiple ingredients, the boundary detection [23], surface normal prediction [12][15][24], and semantic segmentation [26][27] were fused together with depth learning to construct a jointly learning framework. To solve the data insufficiency problem, synthesis data is used to train the depth network [25] [28].

To weak the demand for densely labeled ground truth data during training, a large amount of self-supervised learning methods had emerged [29],[7]. The core idea is to generate a differentiable warping between adjacent views and use photometric error as indirect supervision. This has been successfully applied to optical flow estimation [31],[32][43]. Along this line, several methods [35][44][38] further improve the performance by incorporating additional constraints including ICP regularization [35], epipolar geometric constraints [44], and collaborative competition [46], or better network structures [42]. And later, an online fine-tuning module was proposed to reduce the gap between training and testing [9]. To improve the reliability of depth and pose estimation, some related tasks, such as the optical flow [33][34][46] and semantic segmentation [41][45], were introduced into the self-supervised depth and pose learning framework to constrain the cross-task consistency. To solve the scale inconsistency and ambiguity problem, some recent methods introduced a multi-view geometry consistency [36][37], or replaced the pose network with geometric-based methods[39][40]. To handle occlusions, some works used the forward-backward optical flow consistency to exclude the occlusion areas from the photometric loss computation [33][46][39]. However, the only occlusion estimation used by these methods required bidirectional optical flow estimation, which limited its flexibility. The MaskFlowNet [8] used deformable convolution and an autonomic learned occlusion mask to solve the invalid warping problem in the occlusion areas. To deal with the moving objects, recent works introduced some analytical masks [35][47] and self-discovered masks [36][44] to exclude these invalid regions.

In this work, we introduce a self-supervised learning framework, which aims to integrate the advantages of (a) excellent occlusion aware optical flow estimation; (b) the adaptive cross weighted loss of photometric error and geometric error between optical flow and the scene flow to deal with the moving objects.

III. THE PROPOSED METHODOLOGY

To improve the reliability of the 3D scene understanding, we first introduce to train the MaskFlowNet [8] by an occlusion-aware photometric loss, and then we use the adaptive cross-weighted loss of photometric and geometric error between the depth-pose and optical flow as the optimization objectives. Our goal is to facilitate the self-supervised depth and pose learning from monocular videos by the occlusion aware optical flow, and train them in a fully end-to-end self-supervised manner. Given the unlabeled source frames I_s , where $s \in \{t-1, t+1\}$ and a target frame I_t collected by a moving camera with intrinsic K , we first predict the optical flow $F_{s \rightarrow t}$ between them using the MaskFlowNet. And then we estimate their depth maps (D_t, D_s) using the depth network, the 6DoF camera pose $T_{s \rightarrow t} = [R_{s \rightarrow t}, t_{s \rightarrow t}]$ from the time s to t using the pose network.

A. Self-supervised Learning of Occlusion Self-discovered Optical Flow

The MaskFlowNet [9] is proposed to self-discover the occlusions during the feature matching and achieved state-of-the-art performance in supervised optical flow learning. We will start with the structure of the network. Similar to the PWC-Net [18], multi-scales feature maps of the target frame I_t and source frame I_s are first extracted using a siamese convolutional network. Then, the extracted multi-scales feature maps of the frame I_s at each level l is aligned with the feature map of I_t at level l via a warping operation based on the upsampled flow prediction $F_{t \rightarrow s}^{l+1}$ at level $l+1$. Then a cost volume is computed by a correlation layer, which is subsequently concatenated with the previous extracted feature map of I_t and the upsampled optical flow at level $l+1$. Finally, the residual flow, predicted by the flow estimation layer, is element-wise summation with the upsampled optical flow at level $l+1$ to generate the flow prediction at level l . Iterating this process at all scale levels can predict the multi-scales optical flow.

To deal with the mismatching problem of the correlation layer that occurred at the occluded areas, a learnable occlusion-aware mask called asymmetric occlusion-aware feature matching module is incorporated into the structure

mentioned above. The warped feature tensor of shape (B, C, H, W) is element wise multiplied by the learnable occlusion mask M_{occ} of shape $(B, 1, H, W)$ and then added with an additional trade-off feature tensor μ of shape (B, C, H, W) to facilitate the learning process. M_{occ} is normalized to be within the range of $[0, 1]$. While the warping operation is replaced by the deformable convolution to deal with the asymmetry of the feature matching process in the occluded areas. The learned occlusion mask can also be used to deal with the occlusions in self-supervised depth-pose learning

In this paper, we try to train the occlusion discovered optical flow network in the self-supervised manner by an occlusion aware photometric loss. The photometric loss is widely used in self-supervised learning which measures the difference between the actual collected image and the synthesized image. Referring to the commonly applied self-supervised optical flow learning strategy, we train the optical flow network by combining the temporal supplemental information and the consistency between the optical flow and its inverse flow to exclude the valid supervision information at occlusion area. Given the forward optical flow $F_{t \rightarrow s}$ and the backward optical flow $F_{s \rightarrow t}$, we can use the backward optical flow to generate an occlusion map $M_{t \rightarrow s} \in R^{B \times 1 \times W \times H}$ by modeling the non-occluded area in I_t as the range of $F_{s \rightarrow t}$, which can be calculated by

$$R(x, y) = \sum_{i=1}^w \sum_{j=1}^h \max(0, 1 - |x - (i + F_{s \rightarrow t}^x(i, j))| \cdot \max(0, 1 - |y - (j + F_{s \rightarrow t}^y(i, j))|) \quad (1)$$

Where $R(x, y)$ is the range value at position (x, y) indicating the number of correspondences between adjacent images [32], (W, H) are width and height of optical flow. $F_{s \rightarrow t}^x$ and $F_{s \rightarrow t}^y$ are the horizontal and vertical components of $F_{s \rightarrow t}$. Thus the occlusion map $M_{t \rightarrow s}(x, y) = \min(1, R(x, y))$. As the scene in the two moments $t-1$ and $t+1$ are usually complementary, we also utilize the adaptive loss between the photometric errors L_{bo} and L_{fo} of the two directions $t \rightarrow t-1$ and $t \rightarrow t+1$ to improve the reliability of the algorithm. Instead of using the minimum of the two error, here we use a soft weight computed by the Softmax function. Thus the total occlusion aware photometric loss for optical flow learning can be expressed as

$$L_{op} = \omega_{bo} M_{t \rightarrow t-1} L_{bo} + \omega_{fo} M_{t \rightarrow t+1} L_{fo} \quad (2)$$

Where L_{bo} and L_{fo} are the photometric losses defined as the convex combination of the L1 norm and SSIM. The adaptive per-pixel weights ω_{bo} and ω_{fo} are calculated by the Softmax function according to the relative magnitude of L_{bo} and L_{fo} :

$$\omega_{bo} = e^{(1 - e^{L_{bo}} / (e^{L_{bo}} + e^{L_{fo}})) - 0.5} \quad (3)$$

And ω_{fo} can be computed in the same way. If L_{bo} and L_{fo} are closer, the weights ω_{bo} and ω_{fo} will be close to 1 and correspond to be a non-occluded region. On the contrary, the weights ω_{bo} and ω_{fo} will prone to be zero, and the occlusion is more likely to occur in one direction.

B. Adaptive Cross Weighted Loss Between Depth-pose and Optical Flow

In this section, we describe the loss used for the self-supervised learning of depth, camera pose and optical flow. These tasks are interconnected by the scene re-projection. Assuming $p_t = [x, y]$ is a pixel in the target image I_t , with the predicted depth D_t and camera pose $T_{s \rightarrow t}$ then the re-projection coordinates p_s' in the source image I_s of the rigid transformation can be calculated by

$$[p_s', 1] = K T_{s \rightarrow t} D_t(p_t) K^{-1} [p_t, 1]^T \quad (4)$$

The pixels in the source images belong either to regions explained by ego-motion in (4) or by dynamic objects. For scene structures that cannot be explained by the global rigid motion, one can rely on the more flexible optical flow. In this paper, inspired by the adaptive photometric loss in [9], we proposed an adaptive cross weighted loss of photometric and geometric error between the depth-pose and the optical flow to increase the training data of each task and deal with the occlusions by the learned occlusion mask M_{occ} . The adaptive weights simultaneously consider the photometric error and geometric error between the depth-pose and optical. For the photometric loss L_o and L_d of optical flow and depth-pose, we can compute the soft weight for each task by

$$\omega_o = [(1 - e^{L_{bo}} / (e^{L_{bo}} + e^{L_{fo}})) > 0.28] \quad (5)$$

We find that just throwing away the bigger error during depth-pose and optical flow jointly training will achieve a better performance than (3). As the photometric loss is not reliable in the situations such as illumination variation, reflective surfaces, repetitive textures, here we further introduce the epipolar geometry to improve the robustness of the model. The depth and pose estimation can reduce the rigid flow between adjacent views, thus the epipolar geometric loss between depth-pose and optical flow can also be used to distinguish the motion regions.

To verify the displacements of the rigid flow and optical flow simultaneously by the geometric constraints and distinguish the moving objects, here we incorporate the adaptive weighted epipolar geometric constraints between the depth-pose and optical flow to adaptively mask out bad matches and non-rigid regions. The epipolar geometric constraints for optical flow and rigid flow based on the camera pose are L_{Eo} and L_{Ed} which can be calculated by

$$L_{Ed} = [p_s', 1] F [p_t, 1]^T \quad (6)$$

TABLE I. QUANTITATIVE RESULTS COMPARED WITH THE STATE-OF-THE-ART DEPTH-POSE LEARNING METHODS (WITHOUT POST-PROCESSING[6]) FOR MONOCULAR DEPTH ESTIMATION ON KITTI [1] DATASET WITH EIGEN’S SPLITS AND DEPTH CAPPED AT 80M.

	Methods	Supervision	Error metric				Accuracy metric		
			<i>Abs Rel</i>	<i>Sq Rel</i>	<i>RMSE</i>	<i>RMSE log</i>	$\delta < 1.25$	$\delta < 1.25^2$	$\delta < 1.25^3$
Trained on KITTI	Zhou <i>et al.</i> [7]	M	0.198	1.836	6.565	0.275	0.718	0.901	0.960
	Godard <i>et al.</i> [6]	S	0.141	1.186	5.677	0.238	0.809	0.928	0.969
	Vid2depth [35]	M	0.159	1.231	5.912	0.243	0.784	0.923	0.970
	Yin <i>et al.</i> [33]	M	0.149	1.060	5.567	0.226	0.796	0.935	0.975
	Shen <i>et al.</i> [44]	M	0.139	0.964	5.309	0.215	0.818	0.941	0.977
	Zhan <i>et al.</i> [30]	S	0.135	1.132	5.585	0.229	0.820	0.933	0.971
	Monodepth2 [47]	M	0.115	0.903	4.863	0.193	0.877	0.959	0.981
	Chen <i>et al.</i> [9]	M	0.135	1.070	5.230	0.210	0.841	0.948	0.980
	Xue <i>et al.</i> [37]	M	0.113	0.864	4.812	0.191	0.877	0.960	0.981
	Baseline	M	0.120	0.928	5.034	0.196	0.852	0.951	0.977
	Baseline+MaskFlow	M	0.114	0.876	4.868	0.190	0.877	0.959	0.982
	+cross weights	M	0.112	0.825	4.752	0.188	0.878	0.960	0.982
Trained on Cityscapes	GeoNet.[33]	M	0.210	1.723	6.595	0.281	0.681	0.891	0.960
	Casser <i>et al.</i> [45]	M	0.153	1.109	5.557	0.227	0.796	0.934	0.975
	GLNet. [9]	M	0.129	1.044	5.361	0.212	0.843	0.938	0.976
	Ours	M	0.119	0.986	5.182	0.179	0.852	0.945	0.978

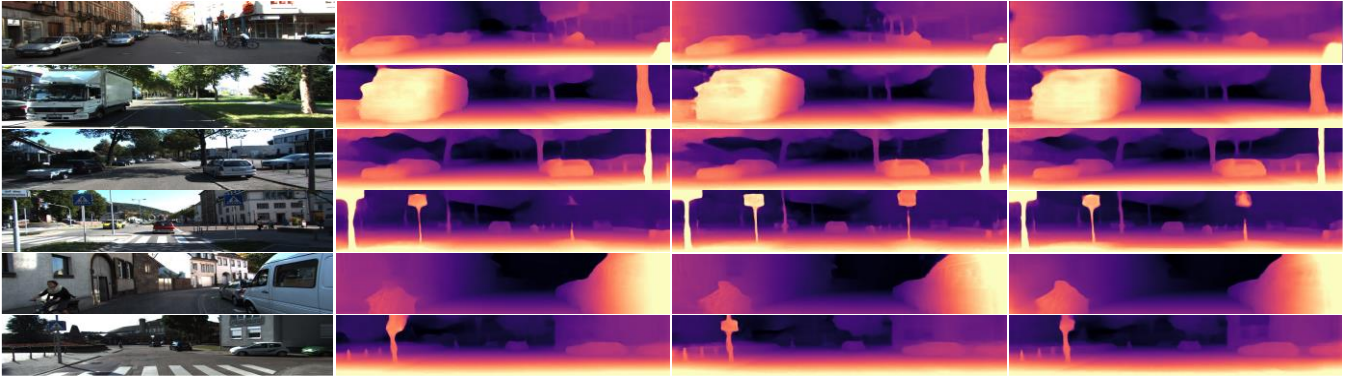


Fig. 2. Qualitative results of depth estimation on KITTI dataset. The columns from left to right show respectively input images, the state-of-the-art predicted depth maps (Godard *et al.*, 2019 [47]; Xue *et al.*, 2020 [36]), and the depths maps obtained by our proposed architecture.

where $F = t_{s \rightarrow t} \times R_{s \rightarrow t}$ is the fundamental matrix. Thus the adaptive weights of geometric constraints for the rigid flow and the optical flow can be computed by (4). To improve the reliability of the above adaptive weighted loss, we use both the weights of photometric error and geometric error to constrain each loss. Thus, the cross weighted loss of the photometric and geometric error between the depth-pose and optical flow is

$$L_{ap} = \omega_{Ed} \omega_o (L_o + \lambda_{ed} L_{Ed}) + \omega_{Eo} \omega_d (L_d + \lambda_{eo} L_{Eo}) \quad (7)$$

The reason behind this is that for a non-rigid object, even if the pixel is properly projected according to the camera’s ego-motion, the photometric error would still be high but the geometric distance under the fundamental matrix F obtained by the estimated camera pose would be proper. While the photometric error of the optical flow is proper for the non-rigid object but the epipolar geometric loss based on the camera pose would be high. To ensure that such pixels are given low weights, we weigh them with their epipolar distance and photometric error compared with rigid flow and optical flow. Thus the total losses are a weighted sum over losses mentioned above, and sum over all valid image pixels.

$$L_{total} = L_{op} + L_{ap} + \lambda_s L_s \quad (8)$$

Where L_s is the smoothness loss [47], λ_s is the weight factor of this loss. These networks are trained jointly in an end-to-end manner. Compared to those works, our method explicitly handles occlusion, moving objects and bad matches.

IV. EXPERIMENTS

In this section, we evaluate the performance of our approach and compare it with prior state-of-the-art approaches on optical flow, depth, and camera pose estimation.

A. Implementation Details

Datasets. We mainly conduct extensive experiments on the benchmarking KITTI [1] and Cityscapes datasets [3], then validate the camera pose estimation on KITTI Odometry Dataset. We used the ground-truth labels provided with the official for evaluation. We additionally trained the model on Cityscapes [3] and tested on KITTI [1], and studied how well the proposed models transfer across datasets. We also use the Make3D dataset [3] to demonstrate the robustness and generalization ability of our proposed method. For the raw KITTI dataset, we use Eigen *et al.*’s split [8] of the raw dataset for training and testing, which is consistent with related works [9][47][37] and the input images are resized to 192×640 , and the optical flow network on KITTI 2015 [1] training set. For the KITTI odometry dataset, we follow the standard setting of using sequences 00-08 for training and 09-10 for testing [39][40]. Since the camera poses in the KITTI odometry dataset are relatively regular and steady, we sample the original test sequences to shorter versions, mimicking fast camera motions, for testing the generalization ability of networks on unseen data.

Parameters setting. For all the experiments, we set the weighting of the different loss components as $\lambda_{eo} = 0.02$ and

TABLE II. OPTICAL FLOW ESTIMATION RESULTS ON KITTI 2015 TRAINING SET. WE REPORT THE AVERAGE END-POINT-ERROR (EPE) ON NON-OCCLUDED REGIONS AND OVERALL REGIONS, FOLLOWING [9].

Methods	Noc	All
UnFlow [31]	-	8.10
GeoNet [33]	8.05	10.81
DF-Net [30]	-	8.98
CC [46]	-	5.66
GLNet [9]	4.86	8.35
MaskFlowNet+ L_{op}	4.35	8.13
MaskFlowNet+ L_{op} + L_{Eo}	4.27	6.60

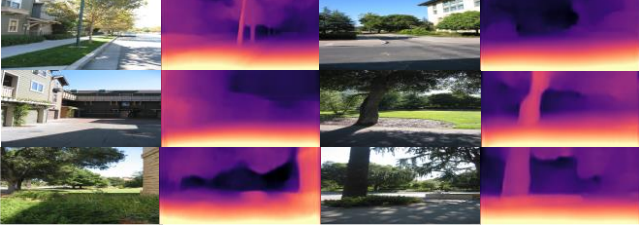


Fig. 3. Illustration of the samples of depth predictions on the Make3D dataset. Note that our model is only trained on the KITTI dataset, and directly tested on Make3D.

$\lambda_{ed}=0.002$ in (7), and $\lambda_s=0.001$ in (8). During training, batch normalization was used for all the layers except the output layers. We trained our model with the Adam optimizer with $\beta_1=0.9$, $\beta_2=0.999$, Gaussian random initialization, and mini-batch size of 6. The learning rate was initially set to 0.0001 and halved it after every 10 epoch until the end. Additionally, random resizing, cropping, flipping and color jittering were used for data augmentation during training following [47]. The backbone network was initialized with ImageNet [22] weights, and we optimized the network for maximum of 30 epochs.

Network Architectures. Since our work focused on a better self-supervised depth-pose learning scheme, we adopt similar depth and optical flow network structures in the existing methods[8][47]. For the depth network, we used the same architecture as [47] which adopts ResNet18 [19] as encoder. The optical flow network was based on MaskFlowNet [9] and trained with the occlusion-aware photometric loss. The camera pose network was similar as in [47]. Firstly, we only trained the optical flow network in a self-supervised manner via occlusion aware photometric loss. After 10 epochs, we froze optical flow network and trained the depth and pose networks for another 10 epochs. Finally, we jointly trained all networks for last 10 epochs. In all experiments, the model in [9] and the minimum of the epipolar geometric loss among source views was used as the baseline.

B. Evaluation of Depth Estimation

Main Results on KITTI. The evaluation of depth estimation follows previous works [9][47]. For a fair comparison, we provided a comparison with the baseline, as well as recent state-of-the-art methods. The measure criterion conformed to the one used in [47]. As shown in Table I, with the same underlying network structure, the proposed method achieved better performance than the state-of-the-art methods. Qualitative results compared with the predictions could be seen in Fig. 2. It is shown that our method could reduce artifacts in low-texture regions of the image and improve the visual quality of the depth map. The proposed adaptive cross-weighted loss can significantly improve both the depth and the

TABLE III. TABLE TYPE STYLES ODOMETRY RESULTS ON THE KITTI [1] ODOMETRY DATASET. RESULTS SHOW THE AVERAGE ABSOLUTE TRAJECTORY ERROR, AND STANDARD DEVIATION, IN METERS.

Methods	Sequence 09	Sequence 10	# frames
Zhou [7]	0.021 \pm 0.017	0.020 \pm 0.015	5
Mahjourian [35]	0.013 \pm 0.010	0.012 \pm 0.011	3
GeoNet [33]	0.012 \pm 0.007	0.012 \pm 0.009	5
Ranjan [46]	0.012 \pm 0.007	0.012 \pm 0.008	5
Monodepth2[47]	0.017 \pm 0.008	0.015 \pm 0.010	2
Shen et al. [44]	0.009 \pm 0.005	0.008 \pm 0.007	3
GLNet [9]	0.011 \pm 0.006	0.011 \pm 0.009	3
Ours	0.008 \pm 0.005	0.008 \pm 0.006	3

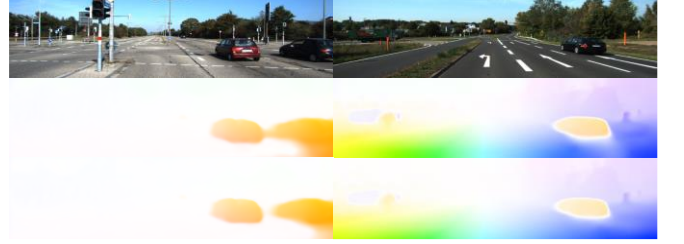


Fig. 4. Qualitative results of flow estimation. Top Row: Input images, Middle Row: MaskFlowNet trained by (2), Bottom Row: joint learning by (7).

optical flow performance. However, the improvement for depth estimation is not as significant as optical flow estimation.

Generalization ability on Make3D. To illustrate that the proposed method was able to generalize to other datasets unseen, we used our network trained only on the KITTI dataset, despite the dissimilarities of the datasets both in contents and camera parameters, we still achieved reasonable results. Qualitative results were shown in Fig. 4, these results would be improved with more relevant training data.

C. Pose Evaluation

We further evaluated our method for visual odometry applications. We compared our method with other state-of-the-art depth-pose learning methods [7][33][9][46] on the official KITTI odometry benchmark. We measured the Absolute Trajectory Error (ATE) over N-frame snippets (N=3 or 5), as measured in [47]. The estimation results in Table II showed the improvement over existing methods with the adaptive cross-weighted loss, we achieved certain performance improvements over state-of-the-art self-supervised depth-pose learning methods.

D. Optical Flow Evaluation

Similar to previous methods [9][39], we used the training set for evaluation, as the optical flow in this paper was learned by self-supervised manner. Table III summarized the results of optical flow estimation using the average end-point-error (EPE) over non-occluded regions (Noc) and overall regions (All) on KITTI 2015 training set. Results showed that the MaskFlowNet [8] could also be well learned by the occlusion aware photometric loss and outperformed most previous self-supervised flow estimation methods [32] [31][43]. Qualitative results were provided in Fig. 3, where we observed that the flow quality was improved for rigidly and non-rigidly moving scene regions.

V. EXPERIMENTS

We have presented an occlusion aware optical flow-guided self-supervised depth-pose learning framework to jointly learn depth, optical flow and camera pose from

monocular videos. The model combines a learnable occlusion mask and novel cross weighted loss of photometric and geometric error between the depth-pose and optical flow to solve the problems of occlusion and the moving objects. This supports the conclusion that geometric information represents a valuable regularization in a transfer learning setting. And the combination of the photometric loss and epipolar geometric constraints can achieve competitive performance with the state-of-the-art methods.

REFERENCES

- [1] A. Geiger, P. Lenz, and R. Urtasun, et al. Are we ready for autonomous driving? the KITTI vision benchmark suite. In *CVPR*, 2012, pp. 3354–3361.
- [2] A. Saxena, M. Sun, and Andrew Y Ng. Make3d: Learning 3d scene structure from a single still image. *PAMI*, 2009.
- [3] M. Cordts, M. Omran, S. Ramos, T. Rehfeld, M. Enzweiler, R. Benenson, U. Franke, S. Roth, and B. Schiele. The Cityscapes dataset for semantic urban scene understanding. In *CVPR*, 2016.
- [4] B. Triggs, P.F. McLauchlan, R. I. Hartley, and A.W. Fitzgibbon. Bundle adjustment a modern synthesis. In *International workshop on vision algorithms*, pages 298–372. Springer, 1999.
- [5] C. Wu. VisualSFM: A visual structure from motion system. 2011.
- [6] C. Godard, O. M. Aodha, and G. J Brostow. Unsupervised monocular depth estimation with left-right consistency. In *CVPR*, 2017.
- [7] T. Zhou, M. Brown, N. Snavely, and D. G Lowe. Unsupervised learning of depth and ego-motion from video. In *CVPR*, 2017.
- [8] S. Zhao, Y. Sheng, Y. Dong, E. I.-C. Chang and Y. Xu, MaskFlowNet: Asymmetric Feature Matching With Learnable Occlusion Mask. In *2020 IEEE/CVF Conference on Computer Vision and Pattern Recognition (CVPR)*, Seattle, WA, USA, 2020, pp. 6277–6286.
- [9] Y. Chen, C. Schmid, C. Sminchisescu. Self-supervised learning with geometric constraints in monocular video: Connecting flow, depth, and camera. In: *Proceedings of the IEEE International Conference on Computer Vision*. pp. 7063–7072 (2019)
- [10] K. Xian, J. Zhang, J. , Wang, O. , Mai, L. , & Cao, Z. . (2020). Structure-Guided Ranking Loss for Single Image Depth Prediction. *IEEE/CVF Conference on Computer Vision and Pattern Recognition (CVPR)*. 2020, pp. 608–617.
- [11] Q. Zhou, T. Sattler, M. Pollefeys and L. Leal-Taix é To Learn or Not to Learn: Visual Localization from Essential Matrices. In *2020 IEEE International Conference on Robotics and Automation (ICRA)*, Paris, France, 2020, pp. 3319–3326.
- [12] D. Eigen and R. Fergus. Predicting depth, surface normals and semantic labels with a common multi-scale convolutional architecture. In *ICCV*, 2015.
- [13] D. Eigen, C. Puhrsch, and R. Fergus. Depth map prediction from a single image using a multi-scale deep network. In *NIPS*, 2014.
- [14] I. Laina, C. Rupprecht, V. Belagiannis, F. Tombari, and N. Navab. Deeper depth prediction with fully convolutional residual networks. In *3DV*, 2016.
- [15] B. Li, C. Shen, Y. Dai, A. V. D. Hengel, and M. He. Depth and surface normal estimation from monocular images using regression on deep features and hierarchical CRFs. In *CVPR*, 2015.
- [16] A. Dosovitskiy, P. Fischer, E. Ilg, P. Hausser, C. Hazirbas, V. Golkov, P. V. D. Smagt, D. Cremers, and T. Brox. FlowNet: Learning optical flow with convolutional networks. In *ICCV*, 2015.
- [17] E. Ilg, N. Mayer, T. Saikia, M. Keuper, A. Dosovitskiy, and T. Brox. FlowNet 2.0: Evolution of optical flow estimation with deep networks. In *CVPR*, 2017.
- [18] D. Sun, X. Yang, M. Liu, and J. Kautz. PWC-net: CNNs for optical flow using pyramid, warping, and cost volume. In *CVPR*, 2018.
- [19] K. He, X. Zhang, S. Ren, and J. Sun. Deep residual learning for image recognition. In *Proceedings of the IEEE conference on computer vision and pattern recognition*, pp. 770–778, 2016.
- [20] Alex Kendall and Roberto Cipolla. Modelling uncertainty in deep learning for camera relocation. In *ICRA*, 2016.
- [21] Alex Kendall and Roberto Cipolla. Geometric loss functions for camera pose regression with deep learning. In *CVPR*, 2017.
- [22] Jia Deng, Wei Dong, Richard Socher, Li-Jia Li, Kai Li, and Li Fei-Fei. Imagenet: A large-scale hierarchical image database. In *2009 IEEE conference on computer vision and pattern recognition*, pp. 248–255. Ieee, 2009.
- [23] E. Ilg, T. Saikia, M. Keuper, and T. Brox. Occlusions, motion and depth boundaries with a generic network for disparity, optical flow or scene flow estimation. In *ECCV*, 2018.
- [24] Bo Li, Chunhua Shen, Yuchao Dai, Anton Van Den Hengel, and Mingyi He. Depth and surface normal estimation from monocular images using regression on deep features and hierarchical CRFs. In *CVPR*, 2015.
- [25] Y. Chen, W. Li, X. Chen, and L. V. Gool. Learning semantic segmentation from synthetic data: A geometrically guided input-output adaptation approach. In *CVPR*, 2019.
- [26] Dan Xu, Wanli Ouyang, Xiaogang Wang, and Nicu Sebe. PAD-net: Multi-tasks guided prediction-and-distillation network for simultaneous depth estimation and scene parsing. In *CVPR*, 2018.
- [27] Zhenyu Zhang, Zhen Cui, Chunyan Xu, Zequn Jie, Xiang Li, and Jian Yang. Joint task-recursive learning for semantic segmentation and depth estimation. In *ECCV*, 2018.
- [28] Nikolaus Mayer, Eddy Ilg, Philip Hausser, Philipp Fischer, Daniel Cremers, Alexey Dosovitskiy, and Thomas Brox. A large dataset to train convolutional networks for disparity, optical flow, and scene flow estimation. In *CVPR*, 2016.
- [29] Ravi Garg, Vijay Kumar BG, Gustavo Carneiro, and Ian Reid. Unsupervised CNN for single view depth estimation: Geometry to the rescue. In *ECCV*, 2016.
- [30] Huangying Zhan, Ravi Garg, Chamara Saroj Weerasekera, Kejie Li, Harsh Agarwal, and Ian Reid. Unsupervised learning of monocular depth estimation and visual odometry with deep feature reconstruction. In *CVPR*, 2018.
- [31] S. Meister, J. Hur, and S. Roth. UnFlow: Unsupervised learning of optical flow with a bidirectional census loss. In *AAAI*, 2018.
- [32] Y. Wang, Y. Yang, Z. Yang, L. Zhao, P. Wang, and W. Xu. Occlusion aware unsupervised learning of optical flow. In *CVPR*, pages 4884–4893, 2018.
- [33] Z. Yin and J. Shi. Geonet: Unsupervised learning of dense depth, optical flow and camera pose. In *CVPR*, pages 1983–1992, 2018.
- [34] Y. Zou, Z. Luo, and J. Huang. Df-net: Unsupervised joint learning of depth and flow using cross-task consistency. In *ECCV*, pages 36–53, 2018.
- [35] R. Mahjourian, M. Wicke, and A. Angelova. Unsupervised learning of depth and ego-motion from monocular video using 3d geometric constraints. In *CVPR*, pages 5667–5675, 2018.
- [36] J. Bian, Z. Li, N. Wang, H. Zhan, C. Shen, M. Cheng, and I. Reid. Unsupervised scale-consistent depth and ego-motion learning from monocular video. In *NeurIPS*, pages 35–45, 2019.
- [37] F. Xue, G. Zhuo, Z. Huang, W. Fu, Z. Wu and M. H. Ang, "Toward Hierarchical Self-Supervised Monocular Absolute Depth Estimation for Autonomous Driving Applications," *2020 IEEE/RSJ International Conference on Intelligent Robots and Systems (IROS)*, Las Vegas, NV, USA, 2020, pp. 2330–2337.
- [38] C. Luo, Z. Yang, P. Wang, Y. Wang, W. Xu, R. Nevatia, and A. Yuille. Every pixel counts++: Joint learning of geometry and motion with 3d holistic understanding. *Tpami*, 2018.
- [39] W. Zhao, S. Liu, Y. Shu and Y.-J. Liu. Towards Better Generalization: Joint Depth-Pose Learning Without PoseNet. In *2020 IEEE/CVF Conference on Computer Vision and Pattern Recognition (CVPR)*, Seattle, WA, USA, 2020, pp. 9148–9158, doi: 10.1109/CVPR42600.2020.00917.
- [40] H. Zhan, C. S. Weerasekera, J. Bian, and I. Reid. "Visual odometry revisited: What should be learnt?" *ICRA-2020*
- [41] Y. Meng et al., "SIGNet: Semantic Instance Aided Unsupervised 3D Geometry Perception," *2019 IEEE/CVF Conference on Computer Vision and Pattern Recognition (CVPR)*, Long Beach, CA, USA, 2019, pp. 9802–9812, doi: 10.1109/CVPR.2019.01004.
- [42] V. Guizilini, R. Ambrus, S. Pillai, A. Raventos, A. Gaidon. 3d packing for self-supervised monocular depth estimation. In: *IEEE/CVF Conference on Computer Vision and Pattern Recognition*. (2020)
- [43] J. Li, J. Zhao, S. Song, T. Feng: Occlusion aware unsupervised learning of optical flow from video. *Proceedings Volume 11605, Thirteenth International Conference on Machine Vision*. (2021)
- [44] T. Shen, et al. Beyond photometric loss for self-supervised ego-motion estimation. *IEEE International Conference on Robotics and Automation (ICRA)*, (2019)

- [45] V. Casser, S. Pirk, R. Mahjourian, A. Angelova: Unsupervised Monocular Depth and Ego-motion Learning with Structure and Semantics. CVPR Workshop on Visual Odometry & Computer Vision Applications Based on Location Clues (VOCVALC), 2019.
- [46] A. Ranjan, V. Jampani, L. Balles, K. Kim, D. Sun, J. Wulff, M.J. Black. Competitive collaboration: Joint unsupervised learning of depth, camera motion, optical flow and motion segmentation. In: Proceedings of the IEEE Conference on Computer Vision and Pattern Recognition. pp. 12240–12249 (2019)
- [47] C. Godard, O. Mac Aodha, M. Firman, G.J. Brostow,: Digging into self-supervised monocular depth estimation. In: Proceedings of the IEEE International Conference on Computer Vision. pp. 3828–3838 (2019)